Joint Estimation of Volume and Velocity in TomoPIV

Ioana Barbu, Cédric Herzet, Etienne Mémin

10TH INTERNATIONAL SYMPOSIUM ON PARTICLE IMAGE VELOCIMETRY - PIV13
Delft, The Netherlands, July 1-3, 2013

Joint Estimation of Volume and Velocity in TomoPIV

Ioana Barbu[1], Cédric Herzet[1] and Etienne Mémin[1]

[1]Fluminance, INRIA Centre Rennes - Bretagne Atlantique, Rennes, France
ioana.barbu@inria.fr

ABSTRACT

A novel formulation of the nexus between instantaneous volumetric reconstruction and velocity retrieval with respect to Tomographic PIV context is presented. In the first part of this paper we relate to the state-of-the-art paradigm and introduce a sequential estimation approach which computes velocity fields out of consecutive 3*D* intensity volumetric distributions. The latter are solutions of ℓ_1-minimization problems which are solved by basis pursuit algorithms. We then express the velocity estimation in a computer vision framework, as a scene flow computation problem. In the second part of the paper we formulate an innovative penalty criterion as an intensity conservation function with respect to both the fluid trajectory and the static volumetric intensity distributions, which allows us to coherently optimize the 3*D* intensity consecutive topologies and their related flow field with regard to their shared structure. The performance is assessed comparing the results from both sequential and joint models with respect to a synthetic tomographic imaging system.

1. Introduction

Our research is motivated by [8], where the authors introduce the Tomographic Particle Image Velocimetry (**TomoPIV**) measurement technique. Their work set the grounds for the estimation of tridimensional (3*D*) motion fields of lightly seeded particles in a turbulent fluid from the images captured by a finite number of cameras disposed around the illuminated volume. The challenge is to accurately reconstruct the 3*D* intensity distribution of a sufficiently large number of seeded particles and their respective velocity fields.

Within the computer vision community, the dense 3*D* vector field representation of the real scene motion is called the **scene flow**, as the term was first coined in [17] by an analogy with **optical flow**. The authors proposed a sequential procedure for its estimation based on the optical flow previously measured in a multiple camera system. However, merging optical flows observed from different viewpoints increases the ambiguities on the sought displacement vector and does not take into account the spatial and temporal dependencies in the images sequence. Recently, procedures oriented towards a joint reconstruction of the structure and of the motion have emerged. The common approach is based on minimizing a global functional which has typically two main terms: *(i) the data term*, which englobes a photometric constraint with respect to the scene motion; *(ii) the spatial term*, which stands for regularizations enforcing known information on the structure of the scene.

The are numerous constraint formulations depending on each application. Valgaerts *et al.* simultaneously compute scene flow and stereo structure provided that only the camera intrinsics are known [16]. Devernay *et al.* compute a sparse scene flow by tracking 3*D* points or surface elements [7]. In [3] the scene flow is regularized using total variation, and in [13] depth sensor is introduces to provide constraints on the motion field. In a nutshell, 3*D* velocity fields are either computed sequentially from an estimation of the scene structure, or based on a model that connects the static and the dynamic information.

The same two reconstruction patterns are identified between the methods used for the retrieval of the scene flow for the TomoPIV application. Elsinga *et al.* [8] sequentially estimate the 3*D* density functions of the scene at two consecutive frames in the video sequence, then compute the the displacement vector between them by means of cross-correlation [14]. Other sequential approaches exploit the information contained by the previously estimated optical flow [5, 15]. Recently, Novara *et al.* presented an enhancement to the classical procedure. The latter models the joint structure of the scene flow and of density function and integrates it to the classical scheme as a first guess for reconstruction algorithm.

Motivated by the advancement in the computer vision field and the TomoPIV community, we propose alternative procedures to both sequential and joint approaches. To this end, we focus on formulating the optimization problems by taking in regard the physical anatomy of the scene.

The paper is organized as follows. In Section 2 we introduce the mathematical abstraction of the tomographic application. In Section 3 present our alternative to current sequential estimation approach, whereas in Section 4 we introduce a formulation which accounts for the nexus between structure and motion. We conclude with a discussion of qualitative results in Section 5.

2. Adopted Model

Let us formulate a mathematical abstraction of the scenario outlined in section 1. For doing so, we first describe the physical continuos signal and relate it to available observations. Then, we present a model for discretizing the $3D$ space and its simultaneous projection on the $2D$ planes.

2.1 Continuous frame

We denote by $w_t(\mathbf{k})$ the density function at time t and position $\mathbf{k} = [k^x, k^y, k^z]^T \in \mathbb{R}^3$ of a passive tracer suspended in the flow. We assume that the density of the passive tracer can be represented as a sum of blurred spheres in the space. Consequently, the $3D$ intensity function can be approximated by a sum of weighted gaussians which account for their evanescent energetic behavior:

$$w_t(\mathbf{k}) = \sum_{j=1}^{M} v_j g_j(\mathbf{k}), \forall \mathbf{k} \in \mathbb{R}^3, v_j \in \mathbb{R}^+, \tag{1}$$

with:

$$g_j(\mathbf{k}) = \exp\Big\{-\frac{\|\mathbf{k}-\mathbf{m}_j\|^2}{2\sigma^2}\Big\}\mathbf{1}\{\|\mathbf{k}-\mathbf{m}_j\| < \varepsilon\}, \forall \mathbf{m}_j \in \mathbb{R}^3, \varepsilon, \sigma^2 \in \mathbb{R}^+$$

where σ^2 is a variance scalar indicating the dispersion from the central tendency parameter located at $\mathbf{m}_j$ with $j = 1,...,M$, where M is the total number of seeded particles, v_j are ponderation weights and $\mathbf{1}\{\cdot\}$ the indicator function which takes 1 if the condition between brackets is respected and 0 otherwise.

The tracer will follow the movements of the fluid and will, consequently, be governed by a displacement function. In fact, we denote by $u(\mathbf{k})$ the displacement at time $t+1$ of a tracer located at position $\mathbf{k} \in \mathbb{R}^3$ at time t. We assume that the density function is invariant along the particle's trajectory. The density constancy over the volume of interest writes:

$$w_{t+1}(\mathbf{k}+u(\mathbf{k})) = w_t(\mathbf{k}), \forall \mathbf{k} \in \mathbb{R}^3. \tag{2}$$

The $3D$ signal simultaneously projects onto the $2D$ planes of the cameras. Each pixel entry i from images at time t represents the integration of the $3D$ light intensity distribution along the cone of view Ω_i originating in the optical center of the camera and passing through the surface of the pixel, as follows:

$$y_{i,t} \approx \int_{\Omega_i} w(\mathbf{k}) d\mathbf{k}, \forall i,t. \tag{3}$$

2.2 Digitized frame

We discretize the $3D$ space visualized by the cameras as a regular polyhedron $\mathcal{V} \subset \mathbb{R}^3$. The latter is defined as a cartesian grid made out of m cubic **vo**lumetric **el**ements (**voxels**) $\zeta_j \subset \mathbb{R}^3$ centered on $\mathbf{k}_j$, $j \in \Gamma = \{1,...,m\}$. We assumed that the density function over $\mathcal{V}$ at time t can be approximated by a piece-wise polynomial function, that is:

$$x_t(\mathbf{k}) = \sum_{j \in \Gamma} p_j(\mathbf{k}) \mathbf{1}\{\|\mathbf{k}-\mathbf{k}_j\|_\infty < \delta/2\} \tag{4}$$

where $p_j(\mathbf{k})$ is an interpolation polynomial which depends on the neighbors of $\mathbf{k}_j$ on the considered $3D$ grid. In the sequel, we will consider interpolation based on triquadratic Lagrange polynomials.

We will exploit (4) to build a finite model approximating (2) and (3). We use the following definitions: $\mathbf{x}_t \doteq \begin{bmatrix} x_t(\mathbf{k}_1) & ... & x_t(\mathbf{k}_m) \end{bmatrix}^T \doteq \begin{bmatrix} x_1 & ... & x_m \end{bmatrix}_t^T$ for $t \in \{0,1\}$, $\mathbf{u} \doteq \begin{bmatrix} u(\mathbf{k}_1) & ... & u(\mathbf{k}_m) \end{bmatrix}^T$ and $\mathbf{x}_1(\mathbf{u}) \doteq \begin{bmatrix} x_1(\mathbf{k}_i + u(\mathbf{k}_i)) \end{bmatrix}_{i \in \Gamma}^T$. Then, using simple algebra, it can be seen that

$$\mathbf{x}_1(\mathbf{u}) = I(\mathbf{u})\mathbf{x}_1, \tag{5}$$

where $I(\mathbf{u})$ is a matrix which explicitly depends on the considered interpolation.

Assuming that $w_t(\mathbf{k}) \simeq x_t(\mathbf{k})$, $t \in \{0,1\}$, and using (5), (2) can be expressed as a density conservation assumption over the discretized grid between two time frames: $\mathbf{x}_0 = I(\mathbf{u})\mathbf{x}_1$. In the sequel, in to account for small changes in the illumination of the scene and interpolation errors, we will slightly relax the latter model as

$$\mathbf{x}_0 = I(\mathbf{u})\mathbf{x}_1 + \mathbf{n}_e, \tag{6}$$

where $\mathbf{n}_e \sim \mathcal{N}(0, \sigma_e^2)$ is a zero-mean Gaussian noise with variance σ_e^2.

Finally, plugging (4) into (3) allows us to formalize the projection model relating the $2D$ observations to the $3D$ discrete intensity distribution at each time frame. Let $\mathbf{y}_t = \begin{bmatrix} y_{1,t} & ... & y_{n,t} \end{bmatrix}^T$ denote the vector collecting the intensities of the n pixels at each time frame $t \in \{0,1\}$. The projection equation then writes $\mathbf{y}_t = \mathbf{D}\mathbf{x}_t$ where matrix $\mathbf{D} \in \mathbb{R}^{n \times m}$ is such that d_{ij} stands for the weight of the contribution of the density in voxel ζ_j to the energy measured within the cone of view passing through the i^{th} pixel. In order to take into account the errors in signal acquisiton, we finally relax to latter model to:

$$\mathbf{y}_t = \mathbf{D}\mathbf{x}_t + \mathbf{n}_t, \forall t \in \{0,1\}, \tag{7}$$

where $\mathbf{n}_t \sim \mathcal{N}(0, \sigma_t^2)$ is a zero-mean Gaussian noise with variance σ_t^2.

3. Sequential Approach

A classical estimation scheme in TomoPIV consists in reconstructing two successive $3D$ intensity distributions of seeded particles and then applying a post-processing procedure for the retrieval of the $3D$ velocity field. We adopt, in this section, the same reconstruction progression. For each of the two steps, we quickly overview the common methods. Finally, we submit our approach and explain its suitability with respect to the physical structure of the real $3D$ scene.

3.1 Sparse Volume Reconstruction

In the current literature, the first step of the sequential estimation paradigm implies the use of methods exploiting positivity and sparsity constraints on the $3D$ signal. The most commonly employed algorithm adopted by the PIV community is the Multiplicative Algebraic Reconstruction Technique (**MART** [9]) which looks for a **non-negative** dense solution under an entropy-based optimization criterion ([8]). Recently, the volumetric estimation problem has been expressed in a **sparse** context in order to enforce the prior that in the visualized volume there is more empty space than seeded particles. The solution is accessed by means of algorithms for sparse reconstruction. In a general form, the criterion writes:

$$\mathbf{x}_t^* = \arg\min_{\mathbf{x}} \|\mathbf{x}\|_0 \text{ subject to } \begin{cases} c_1: & \mathbf{D}\mathbf{x} = \mathbf{y}_t \\ c_2: & x_i \geq 0, \forall i. \end{cases} \tag{8}$$

where $\|\mathbf{x}\|_0$ is the ℓ_0-norm of $\mathbf{x}$ counting the number of non zeros in the latter. The constraint c_1 ensures that the solution verifies the model, while the c_2 constraint ensures the non-negativity on the coefficients x_i of the signal (and is optional). Unfortunately, the ℓ_0-problem is NP-hard. In practice, we need to consider sub-optimal algorithms to access to its solutions. A first family of such algorithms approximates the ℓ_0-norm by the ℓ_1-norm in order to transform the initial problem, non-convex, such that classical optimization schemes (*Basis Pursuit* [6]) can be applied to solve it. This case has been considered in a tomographic scenario by *Petra et al.* in [12]. Another approach consists in resorting to greedy algorithms which aim at solving (8) by making a succession of locally-optimal decisions on the support vector of the sparse decomposition. The performance of several greedy algorithms with respect to the algebraic state-of-the-art procedure and basis pursuit algorithms have been analyzed in [2]. Numerical simulations have showed that the sparsity maximization approach outperforms MART with respect to accuracy [11], [2] in certain operating regimes of interest. These considerations have encouraged us to search for for the non-negative solution which minimizes the ℓ_1-norm on the sought signal.

3.2 Velocity retrieval

In the TomoPIV community, the motion retrieval between the pair of two reconstructed intensity distributions is usually performed by means of $3D$ **cross-correlation**, enhanced by an iterative affine transformation between the interrogation areas [14]. Other motion estimation techniques have been investigated with respect to the tomographic application. We mention [5] where only the planar components of the displacement are estimated and [15], where the retrieval of the 3 components of the velocity vector is performed by means of a scene flow computation procedure within a stereo disposal of the cameras around the volume.

Our motion retrieval procedure relates to the Lucas-Kanade paradigm (**LK**) [1]. The latter algorithm is based on the density conservation constraint such as the one defined in (6). This conservation only introduces one constraint for the estimation of the tree dimensional displacement vector. This limitation is widely known in the computer vision community as the aperture problem. In order to cope with this problem, additional constraints on the sought displacement must be introduced. The LK approach supposes that the displacement $u(\mathbf{k})$ satisfied the density conservation constraint in a small neighborhood around $\mathbf{k}$. More specifically, let $\mathbf{x}_t^*(\mathbf{k})$ be the vector collecting the elements of $\mathbf{x}_t^\star$ in a neighborhood of $\mathbf{k}$. The LK algorithm estimates $u(\mathbf{k})$ as the solution of the following problem:

$$\min_{u(\mathbf{k})} \|\mathbf{x}_0^*(\mathbf{k}) - I(u(\mathbf{k}))\mathbf{x}_1^*(\mathbf{k})\|_2^2, \tag{9}$$

where I is an interpolation matrix. We appeal to an iterative gradient-based descent procedure in order to access to the solution of (9). The elements of the gradient of $J_s(u(\mathbf{k})) \doteq \|\mathbf{x}_0^*(\mathbf{k}) - I(u(\mathbf{k}))\mathbf{x}_1^*(\mathbf{k})\|_2^2$ writes:

$$\frac{\partial J_s(u(\mathbf{k}))}{\partial u^c(\mathbf{k})} = -(\mathbf{x}_0^*(\mathbf{k}) - I(u(\mathbf{k}))\mathbf{x}_1^*(\mathbf{k}))^T \frac{\partial I(u(\mathbf{k}))\mathbf{x}_1^*(\mathbf{k})}{\partial u^c(\mathbf{k})}, \quad \text{with } c \in \{x, y, z\}.$$

We stress that we access to the values of $\frac{\partial I(u(\mathbf{k}))\mathbf{x}_1^*(\mathbf{k})}{\partial u^c(\mathbf{k})}$ by deriving the analytical function defined in (4) with respect to each component of the displacement vector.

4. Joint Approach

Although conceptually interesting, the sequential procedure suffers from some possible drawbacks:

- the reconstruction of the $3D$ density function is performed independently of the temporal sequence. In reality, the instantaneous volumetric distributions can be modeled like a $3D$ entity deformed by a displacement (*i.e.*, the fluid flow). Therefore, any information on the displacement field could be taken into account in the reconstruction of the density function.

- The estimation of the displacement field is computed between pairs $3D$ intensity distributions at consecutive time frames. In practice, the quality of these reconstructed volumetric distributions can be affected by the low number of observations and measurement imprecisions. The noise affecting these estimations is not taken into account in the current literature. The velocity estimation algorithms can therefore be improved by accounting for the imprecisions governing the reconstruction of $3D$ density distributions and of the displacement field between them.

The idea is thus to go towards a joint estimation framework. In the TomoPIV context, *Scarano et al.* have recently proposed an enhancement to the classical MART scheme through an iterative procedure whose aim is to initialize the algebraic procedure by a first guess accounting for both successive views of the scene [10]. The so-called motion tracking enhancement (**MTE**) yields better performance with respect to geometric topology of the sought particles.

In the same spirit as this refined estimation paradigm, we aim in this work at proposing a novel global formulation of the nexus between instantaneous volumetric reconstruction and velocity retrieval. More specifically, we consider the following optimization problem:

$$\min_{\mathbf{x}_0(\mathbf{k}),\mathbf{x}_1(\mathbf{k}),u(\mathbf{k})} J(\mathbf{x}_0(\mathbf{k}),\mathbf{x}_1(\mathbf{k}),u(\mathbf{k})), \tag{10}$$

where

$$J(\mathbf{x}_0(\mathbf{k}),\mathbf{x}_1(\mathbf{k}),u(\mathbf{k})) = \frac{\|\mathbf{x}_0(\mathbf{k})-\mathbf{x}_0^*(\mathbf{k})\|_2^2}{\sigma_0^2} + \frac{\|\mathbf{x}_1(\mathbf{k})-\mathbf{x}_1^*(\mathbf{k})\|_2^2}{\sigma_1^2} + \frac{\|\mathbf{x}_0(\mathbf{k})-I(u(\mathbf{k}))\mathbf{x}_1\|_2^2}{\sigma_e^2}, \forall \mathbf{k} \in \mathcal{V}. \tag{11}$$

The first two terms penalize the discrepancies between $\mathbf{x}_t(\mathbf{k})$ and the volume estimated during the volume reconstruction step $\mathbf{x}_t^\star(\mathbf{k})$. The last one enforces the density conservation constraints.

Our strategy to access to the minimum of (10) is based on a sequence of alternative minimization with respect to the vector of pairs $\mathbf{x}_t(\mathbf{k})$ and to $u(\mathbf{k})$:

$$u(\mathbf{k})^{(l+1)} = \arg\min_{\mathbf{u_k}} J(\mathbf{x}_0^{(l)}(\mathbf{k}),\mathbf{x}_1^{(l)}(\mathbf{k}),u(\mathbf{k})), \tag{12}$$

$$(\mathbf{x}_0{}^{(l+1)}(\mathbf{k}),\mathbf{x}_1^{(l+1)}(\mathbf{k})) = \arg\min_{\mathbf{x}_0(\mathbf{k}),\mathbf{x}_1(\mathbf{k})} J(\mathbf{x}_0(\mathbf{k}),\mathbf{x}_1(\mathbf{k}),u^{(l+1)}(\mathbf{k})). \tag{13}$$

where l denotes the iteration number. We note that the first optimization problem (12) is equivalent to (9) since only the last term in (11) depends on $u(\mathbf{k})$. We will therefore resort to the gradient descent technique described in the previous section to look for its minimum. We also consider a gradient procedure to look for the solution of (13). The partial derivatives of $J(\mathbf{x}_0(\mathbf{k}),\mathbf{x}_1(\mathbf{k}),u(\mathbf{k}))$ with respect to the elements of $\mathbf{x}_0(\mathbf{k})$ and $\mathbf{x}_1(\mathbf{k})$ can be efficiently evaluated via the following formulas:

$$\nabla_{\mathbf{x}_0(\mathbf{k})} J(\mathbf{x}_0(\mathbf{k}),\mathbf{x}_1(\mathbf{k}),u(\mathbf{k})) = \frac{1}{\sigma_0^2}(\mathbf{x}_0(\mathbf{k})-\mathbf{x}_0^*(\mathbf{k})) + \frac{1}{\sigma_e^2}(\mathbf{x}_0(\mathbf{k})-I(u(\mathbf{k}))\mathbf{x}_1(\mathbf{k})) \tag{14}$$

$$\nabla_{\mathbf{x}_1(\mathbf{k})} J(\mathbf{x}_0(\mathbf{k}),\mathbf{x}_1(\mathbf{k}),u(\mathbf{k})) = \frac{1}{\sigma_1^2}(\mathbf{x}_1(\mathbf{k})-\mathbf{x}_1^*(\mathbf{k})) + \frac{1}{\sigma_e^2}(-I^T(u(\mathbf{k}))\mathbf{x}_0(\mathbf{k}) + I^T(u(\mathbf{k}))I(u(\mathbf{k}))\mathbf{x}_1(\mathbf{k})) \tag{15}$$

Let us note that our formulation allows for the initial estimation of volume intensity distributions $\mathbf{x}_0^*$, $\mathbf{x}_1^*$ by means of any state-of-the-art procedure, including the ubiquitous MART.

5. Performance Assessment

We consider a cuboid partitioned into a cartesian grid of $61 \times 61 \times 31$ voxels, with voxel unit set at $1mm$. The origin of the scene frame is chosen in the center of the cuboid. We place 4 cameras around the cuboid of interests such that the volume's shape is visible on each sensor; each camera has a CCD sensor of size $10 \times 10mm$, for a 151×151 resolution and a $7.5101mm$ focal distance. The seeding density of the volume is set at 0.02 particles per pixel (ppp). We apply a shear flow in the y dimension with wavelength $L = 120$ to the seeded particles and estimate an initial distribution of the density function by launching the basis pursuit algorithm with non-negative constraints (BP+) and the MART procedure for two consecutive frames. Figure 1 presents the solutions computed on a sub-grid included in the initial cuboid, for a fixed value of the Z dimension. While they both reconstruct positive energies, the solution given by the BP+ procedure is more close to the actual structure of the volume, which contains more empty space than seeded particles.

We proceed to the reconstruction of the displacement fields in a sequential and in a joint scenario. A window of size $5 \times 5 \times 5$ is considered around each grid position. We launch (9) and (10) for each of the initially estimated $3D$ distributions. The performance is assessed by qualitatively observing the mean squared displacement error (Figure 2) and the angular error (Figure 3) which are computed with respect to the known shear flow displacement applied at grid points.

The joint approach slightly impacts on the precision of the estimated displacement between two sparse volume reconstructions (Figure 2 (a,d)). Moreover, we observe clear improvements between velocity estimations when the joint procedure is applied to the density function reconstructed by MART. The same observations are available for Figure 3. Angular precision is improved by the joint procedure with respect to both density reconstruction algorithms, with slightly more significant changes between the MART-initialized distributions. These results point out that the joint approach accounts for errors on the volumetric reconstruction; the iterative updates on the estimations of the density function allows us to correct a poor reconstruction of the volume and, therefore, to perform a more accurate estimation of the displacement fields.

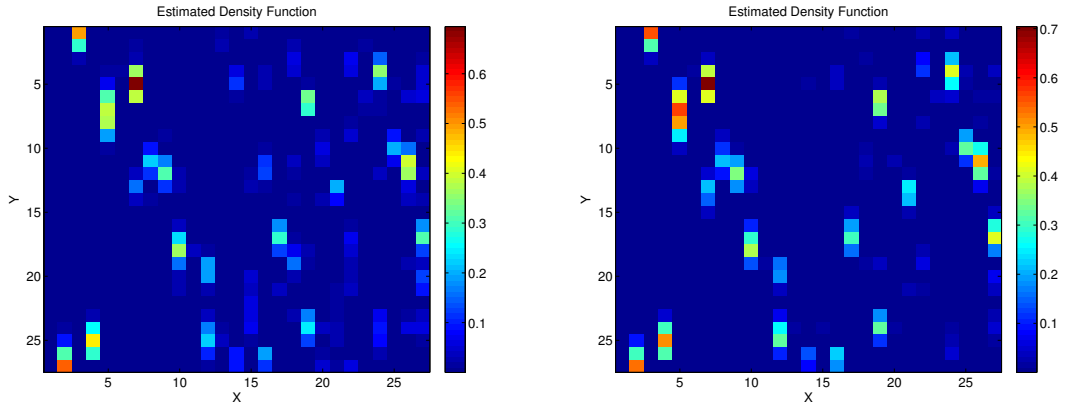

(a) MART (b) BP+

Figure 1: Estimation of the density functions at time frame $t = 0$, computed at $Z = 0$

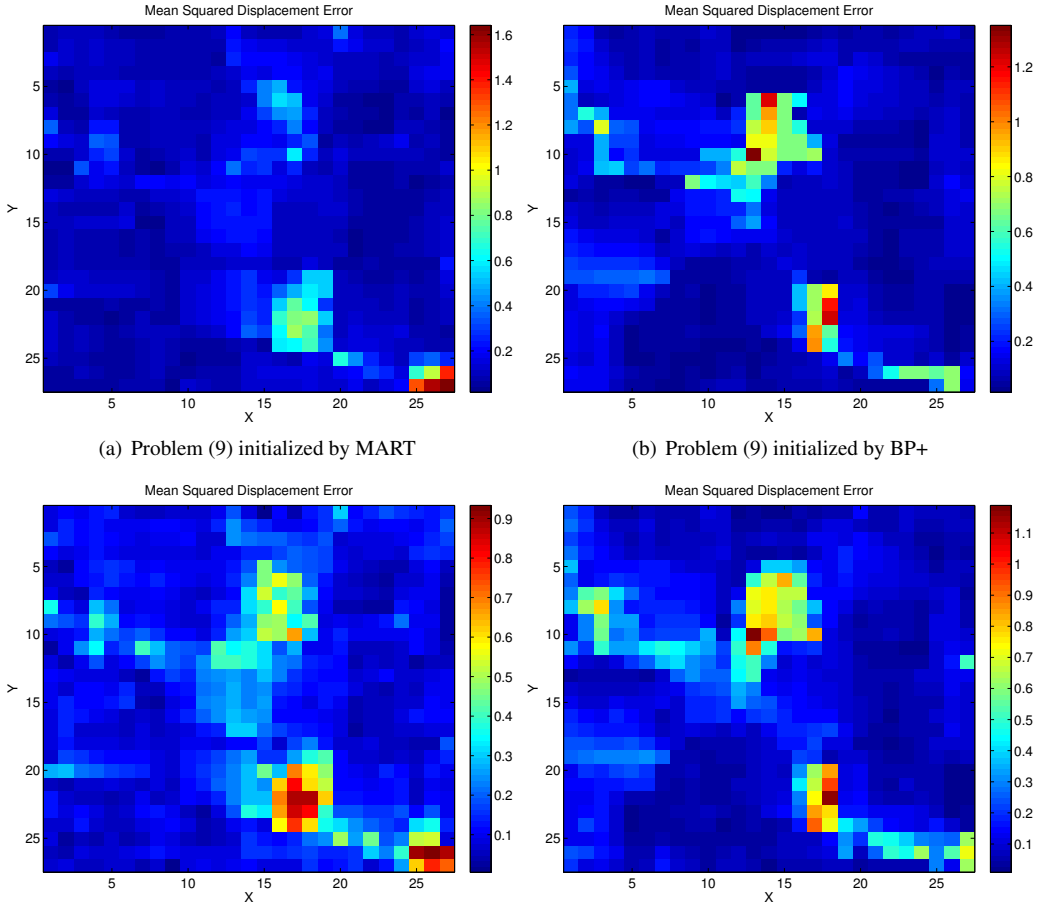

(a) Problem (9) initialized by MART (b) Problem (9) initialized by BP+

(c) Problem (10) initialized by MART (d) Problem (10) initialized by BP+

Figure 2: Mean squared displacement error observed for $Z = 0$.

Future investigations will show comparative results with the commonly employed MTE-MART procedure both in a simulated scenario and on time-resolved experiments.

6. Conclusion

The trend in motion flow estimation is set by the formulation of procedures oriented towards a joint reconstruction of the structure and of the displacement fields. A novel formulation of this joint problem has been presented. The theoretically frame has been presented

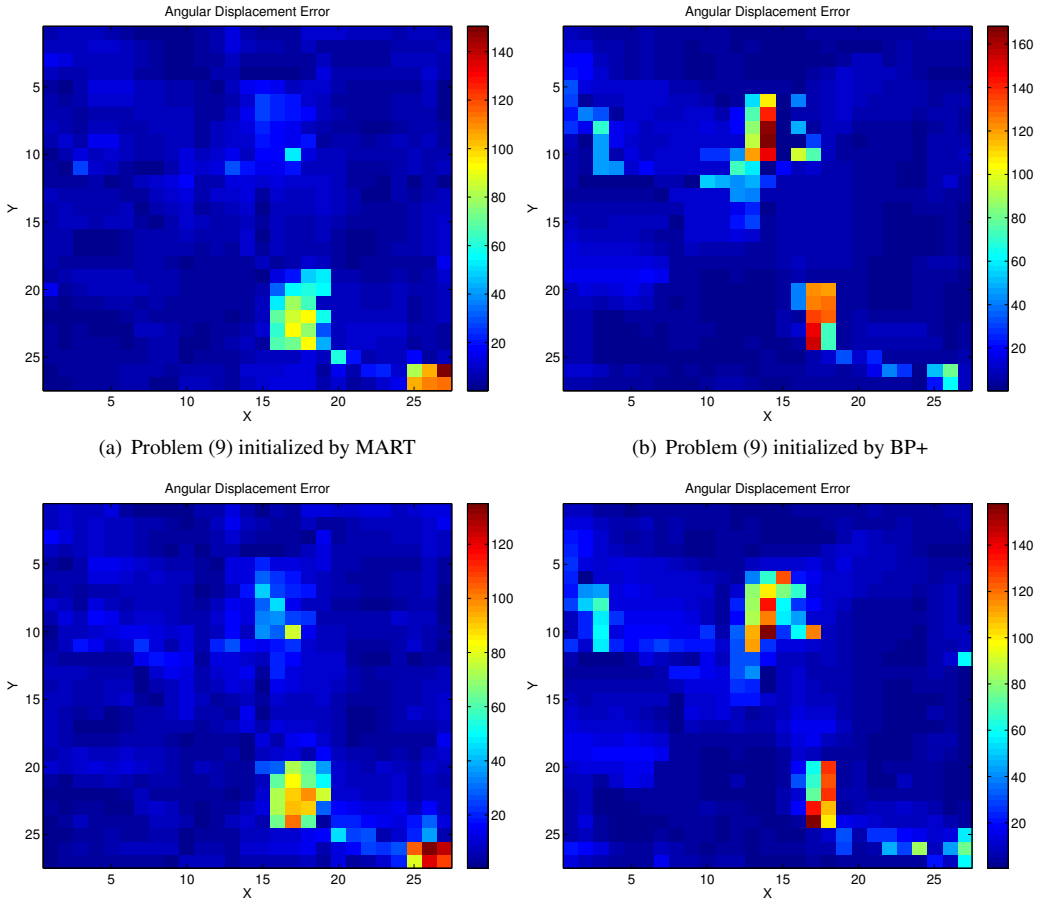

(a) Problem (9) initialized by MART

(b) Problem (9) initialized by BP+

(c) Problem (10) initialized by MART

(d) Problem (10) initialized by BP+

Figure 3: Angular displacement error observed for $Z = 0$.

with connections to the computer vision field, as well as to the TomoPIV community. The performance has been assessed by means of $3D$ simulations. A short comparative study with a more classical sequential reconstruction paradigm acknowledged, for a random average case scenario of the tomographic application, its contributions to a more accurate estimation of the velocity by accounting for noise on poor volume reconstructions. However, its robustness with respect to different characterizations of a real scene (*i.e.*, change in illumination, large displacement fields) is to be verified by intensive experiments on real data. Furthermore, such variables can be accounted for in future work and open the way for the design of a problem formulation closer to the physical anatomy of the scene.

References

[1] S. Baker and I. Matthews. Lucas-Kanade 20 Years On: A Unifying Framework. *INT J COMPUT VISION*, 56(3):221 – 255, March 2004.

[2] I. Barbu, C. Herzet, and E. Mémin. Sparse models and pursuit algorithms for PIV tomography. In *FVR*, 2011.

[3] T Basha, Y. Moses, and N. Kiryati. Multi-view scene flow estimation: A view centered variational approach. In *CVPR*, 2010.

[4] D.P. Bertsekas. *Nonlinear Programming*. Athena Scientific, 1999.

[5] F. Champagnat, A. Plyer, G. Le Besnerais, B. Leclaire, S. Davoust, and Y. Le Sant. Fast and accurate PIV computation using highly parallel iterative correlation maximization. *EXP FLUIDS*, 50(4):1169–1182, 2011.

[6] S. Chen, D. L. Donoho, and M. A. Saunders. Atomic Decomposition by Basis Pursuit. *SIAM J SCI COMPUT*, 20(1):33–61, 1998.

[7] F. Deverney, D. Mateus, and M. Guilbert. Multi-camera scene flow by tracking 3-D points and surfels. In *CCVPR*, 2006.

[8] G. Elsinga, F. Scarano, B. Wieneke, and B. van Oudheusden. Tomographic particle image velocimetry. *EXP FLUIDS*, 41(6):933–947, 2006.

[9] G. T. Herman and A. Lent. Iterative reconstruction algorithms. *COMPUT BIOL MED*, 6:273–294, 1976.

[10] M. Novara, K. J. Batenburg, and F. Scarano. Motion tracking-enhanced MART for tomographic PIV. In *MEAS SCI TECHNOL*, volume 21, 2010.

[11] S. Petra, A. Schröder, and C. Schnörr. 3D Tomography from Few Projections in Experimental Fluid Mechanics. In *Imaging Measurement Methods for Flow Analysis*, volume 106, pages 63–72. 2009.

[12] S. Petra, A. Schröder, B. Wieneke, and C. Schnörr. Tomography from Few Projections in Experimental Fluid Dynamics. In *Imaging Measurement Methods for Flow Analysis*, volume 106, 2009.

[13] Julian Quiroga, Frédéric Devernay, and James Crowley. Scene Flow by Tracking in Intensity and Depth Data. In *CVPRW*, pages 50–57, 2012.

[14] F Scarano and M. L. Riethmuller. Advances in iterative multigrid PIV image processing. *EXP FLUIDS*, 29:51–60, 2000.

[15] M. Stanislas, K. Okamoto, C. Kähler, J. Westerweel, and F Scarano. Main results of the First International PIV Challenge. *EXP FLUIDS*, 45:27–71, 2008.

[16] L. Valgaerts, A. Bruhn, H. Zimmer, J. Weickert, C. Stoll, and C. Theobalt. Joint estimation of motion, structure and geometry from stereo sequences. In *ECCV*, 2010.

[17] S. Vedula, S. Baker, P. Rander, R. T. Collins, and T. Kanade. Three-Dimensional Scene Flow. In *ICCV*, 1999.